Fluorescent Lifetime Quenching near *d* = 1.5 nm Gold Nanoparticles: Probing NSET Validity

T. L. Jennings, M. P. Singh, and G. F. Strouse*

Contribution from the Department of Chemistry and Biochemistry, Florida State University, Tallahassee, Florida 32306-4390

Received December 9, 2005; E-mail: strouse@chem.fsu.edu

Abstract: The fluorescence behavior of molecular dyes at discrete distances from 1.5 nm diameter gold nanoparticles as a function of distance and energy is investigated. Photoluminescence and luminescence lifetime measurements both demonstrate quenching behavior consistent with $1/d^4$ separation distance from dye to the surface of the nanoparticle. In agreement with the model of Persson and Lang, all experimental data show that energy transfer to the metal surface is the dominant quenching mechanism, and the radiative rate is unchanged throughout the experiment.

Introduction

Application of optical molecular rulers to questions in biochemistry, biodiagnostics, and bimolecular imaging allows routine measurement of dynamic distance changes in molecules. We recently demonstrated the applicability of a long-range molecular ruler consisting of an organic dye donating energy to a small (1.4−1.5 nm diameter) gold nanoparticle, termed nanosurface energy transfer (NSET).[1] This technique allowed changes in conformational distances between 2 and 15 nm to be probed for protein−nucleic acid interactions on double-stranded DNA (dsDNA) using optical methods. NSET is similar to Förster resonance energy transfer (FRET); however, the measurable distances are extended nearly 2-fold for optical molecular rulers by following a $1/d^4$ distance dependence. Nanoparticles below the 2 nm scale should be of particular interest for the minimally invasive integration of nanotechnology with biological systems. The intensity quenching mechanism via coupling of the oscillating electronic dipole of a dye to a metal surface with loss of energy via heat analogous to the theoretical treatment developed by Chance, Prock and Silbey,[2] and Persson and Lang[3] for bulk metals.

This theoretical treatment can explain the oscillator coupling to a metallic nanoparticle (NP) with surprisingly good agreement to experimental data,[1] which is unexpected because a 1.5 nm Au NP neither has a significant core nor displays strong surface plasmon resonance (SPR) character. The observation of quenching behavior that follows the theoretical treatment of Persson and Lang for a bulk metal is surprising due to the poorly developed surface in materials below 2 nm. While these systems are above the limit where the crystal field levels split, they are not large enough to express a coherent surface plasmon resonance. This may not be critical if the logic of Ruppin is

applied, where he has theorized that the primary difference between the rates of energy transfer to a plane and to a sphere is manifest in the loss of lifetime oscillations at large distance in the spherical case, due to reduced reflectivity.[4] This implies that an energy transfer mechanism may not be drastically affected by moving from a plane to the spherical acceptor case.

Although the experimental results are consistent with NSET behavior, seemingly contradictory findings for the optical response of molecular dyes interacting with metal NPs have been reported in the literature with both radiative rate enhancement and energy transfer quenching at moderate distances.[5−7] A common theme for most theories relies upon the existence of SPR bands in the metal particle. The lower quantum efficiency of fluorophores near or on metal surfaces has been interpreted in terms of lossy surface waves[8,9] or by suppression of the radiative rate.[5] Under certain conditions, photoluminescence enhancement has been reported and is described as resulting from wavevector matching and coupling to a plasmon for far-field emission via a classical description of light.[6] An interesting question presents itself, therefore, when inquiring about the behavior of a dipole emitter when the metal does not exhibit an SPR band, such as occurs when the metal particle is very small, ≤2 nm.[10] Because 1.5 nm diameter gold NPs do not display surface plasmon character, the only means by which dye quenching will be observed is limited to either a change in the radiative rate (k_r) of the dye or the introduction of an energy transfer rate (k_{et}) to the metal NP. The details of the mechanism

(1) Yun, C. S.; Javier, A.; Jennings, T.; Fisher, M.; Hira, S.; Peterson, S.; Hopkins, B.; Reich, N. O.; Strouse, G. F. *J. Am. Chem. Soc.* **2005**, *127*, 3115−3119.
(2) Chance, R.; Prock, A.; Silbey, R. *Adv. Chem. Phys.* **1978**, *60*, 1−65.
(3) Persson, B. N. J.; Lang, N. D. *Phys. Rev. B* **1982**, *26*, 5409−5415.
(4) Ruppin, R. *J. Chem. Phys.* **1982**, *76*, 1681−1684.
(5) Dulkeith, E.; Ringler, M.; Klar, T. A.; Feldmann, J.; Javier, A. M.; Parak, W. J. *Nano Lett.* **2005**, *5*, 585−589.
(6) Lakowicz, J. R. *Anal. Biochem.* **2005**, *337*, 171−194.
(7) Thomas, K. G.; Kamat, P. V. *J. Am. Chem. Soc.* **2000**, *122*, 2655−2656.
(8) Worthing, P. T.; Amos, R. M.; Barnes, W. L. *Phys. Rev. A* **1999**, *59*, 865−872.
(9) Kalkman, J.; Kuipers, L.; Polman, A.; Gersen, H. *Appl. Phys. Lett.* **2005**, *86*, 041113−1−041113−3.
(10) Logunov, S. L.; Ahmadi, T. S.; El-Sayed, M. A.; Khoury, J. T.; Whetten, R. L. *J. Phys. Chem. B* **1997**, *101*, 3713−3719.

can be probed by correlating the photoluminescence (PL) and lifetime (τ) behavior for a set of dyes, spaced at controlled distances.

The relationship between photoluminescence (PL) intensity and lifetimes is easily shown by considering that

$$\tau_{obs} = \frac{1}{k_{obs}} = \frac{1}{k_r + k_{nr} + k_{et}} \quad (1)$$

and

$$\Phi_{em} = \frac{k_r}{k_r + k_{nr} + k_{et}} = k_r \tau_{obs} \quad (2)$$

where eq 1 states that the observed lifetime, τ_{obs}, is the inverse of all rates of decay, k_{obs}; where k_{obs} is the sum of the radiative rate, k_r, the nonradiative rate, k_{nr}, and the rate of energy transfer, k_{et}. The radiative and nonradiative rates are normally considered constants for a dye under defined conditions, leaving k_{et} as the major contributor to the shortening of an observed lifetime. The rate of energy transfer may be calculated, therefore, from the difference in rates of excited-state de-excitation in the presence and absence of gold quencher:

$$k_{et} = \frac{1}{\tau'_{obs}} - \frac{1}{\tau_{obs}} \quad (3)$$

where τ'_{obs} is the quenched lifetime of the fluorophore. The quantum yield (eq 2) is a convenient measurement relating PL intensity to k_r and the observed lifetime, τ_{obs}. For a high quantum efficiency dye, k_{nr} is very small, and one predicts that a change in k_r will lead to a corresponding change in the observed lifetime of a dye, affecting the measured Φ_{em}. Conversely, energy transfer should lead to a correlated loss in lifetime and intensity for the NP−dye combination. A dilemma is presented by these statements because both a changing k_r and the introduction of an energy transfer pathway (k_{et}) could lead to the observation of quenched PL and a decreased lifetime. How then can one distinguish the true origin of the decreased PL intensity? The purpose of this paper is to demonstrate that the mechanism of PL quenching for an organic dye near a small 1.5 nm NP is almost entirely via energy transfer to the metal surface and that the quenching efficiency is defined by a $1/d^4$ distance dependence, consistent with the predictions of Persson and Lang in an NSET model.

Experimental Section

Nanoparticle Synthesis: Gold nanoparticles were synthesized as described by literature techniques,[11] using the rapid reduction of hydrogen tetrachloroaurate ($AuCl_4\cdot 3H_2O$) in the presence of tetraoctylammonium bromide by sodium borohydride in an argon-sparged water/toluene mixture. TEM measurements displayed particles with an average diameter of 1.5 ± 0.5 nm. The particles were washed thoroughly with a variety of solvents, including hexanes, sodium nitrite solution, and MeOH−H_2O. Ligand exchange was accomplished using ∼400 mg bis(*p*-sulfonatophenyl)phenylphosphine dihydrate (SPP) in 30 mL of Nanopure H_2O to 32 mg of purified nanocrystal in 32 mL of methylene chloride. The two phases were stirred overnight, resulting in extraction of the organically soluble NP to the aqueous phase through

ligand exchange. Aqueous NP was lyophilized into small aliquots of ∼2 nmol/vial and stored at 4 °C.

dsDNA. Nanoparticle Coupling: Complementary DNA strands were purchased with either 5′-C_6-dye or 5′-C_6-SH already HPLC-purified from IDT DNA Technologies. All strands[31] were engineered to minimize secondary structures using mFold. Purity for Cy5-labeled DNA was verified via HPLC analysis (C-4, 300 Å, 10−80% acetonitrile in 45 min). Purity for FAM and thiol-labeled DNA was verified on FPLC (30−90% 1 M NaCl in 0.1 M NaOH over 30 min (≤30mer) or 60 min (>30mer)). A standard assembly of dsDNA with the NP was accomplished by first deprotecting 800 pmol of the single-stranded 5′-thiol DNA with 50 mM tris(2-carboxyethyl)phosphine hydrochloride (TCEP) in 20 mM PBS buffer pH 7.5 at room temperature for 30 min. The freshly deprotected DNA−thiol was desalted with a NAP-5 column, collecting the first 500 μL eluted which contained 75% (600 pmol) of the total DNA loaded onto the column. The dye-containing complementary strand (590 pmol) was immediately added, and the strands were annealed at 95 °C for 2 min, cooled to room temperature for 2 min, and then added to 4 nmol of dry H_2O−soluble NP (NOTE: this is a 1:6.7 stoichiometry dsDNA:NP to ensure predominately 1:1 binding). The mixture was vortexed and placed at 4 °C in the dark for conjugation >24 h. Successive (≥2) ethanol precipitations were performed to purify unbound NP from the dsDNA−NP conjugate. The purified dsDNA−NP conjugate was reconstituted in 20 mM PBS pH 7.5 buffer and stored at 4 °C in the dark.

Absorption/Photoluminescence: Absorption measurements were acquired on a Varian Cary 50 UV−vis spectrophotometer, and photoluminescence measurements were acquired on a Varian Cary Eclipse Fluorescence spectrophotometer using Z-matched 50 μL quartz cuvettes. A typical quantum yield was calculated by measuring the absorption over the 200−800 nm range for both the sample described above and a control (dsDNA−dye without NP), keeping the peak of the dye absorption ≤0.1 au. Continuous-wave photoluminescence (cw-PL) was first measured on the control strand, adjusting the sensitivity to maximize the PL signal. *Under identical settings*, the PL intensity of the dsDNA−NP sample was then measured. Quantum efficiencies of quenching were determined via the following calculation:

$$\Phi_{QEff} = 1 - \frac{I_{sample}}{I_{control}} \times \frac{A_{control}}{A_{sample}} \quad (4)$$

where Φ_{QEff} is the quantum efficiency of energy transfer, $I_{sample,control}$ is

(12) Hays, J. B.; Magar, M. E.; Zimm, B. H. *Biopolymers* **1969**, *8*, 531.
(13) Persson, B. N. *J. Solid State Commun.* **1978**, *27*, 417−421.
(14) Persson, B. N. J. *Surf. Sci.* **1993**, *281*, 153−162.
(15) Kuhn, H. *J. Chem. Phys.* **1970**, *53*, 101.
(16) Chew, H. *J. Chem. Phys.* **1987**, *87*, 1355−1360.
(17) Leung, P. T. *Phys. Rev. B* **1990**, *42*, 7622−7625.
(18) Chang, R. L. *Opt. Commun.* **2005**, *249*, 329−337.
(19) Gersten, J.; Nitzan, A. *J. Chem. Phys.* **1981**, *75*, 1139−1152.
(20) Gersten, J. I.; Nitzan, A. *Chem. Phys. Lett.* **1984**, *104*, 31−37.
(21) Gersten, J. I.; Nitzan, A. *Surf. Sci.* **1985**, *158*, 165−189.
(22) Dulkeith, E.; Morteani, A. C.; Niedereichholz, T.; Klar, T. A.; Feldmann, J.; Levi, S. A.; van Veggel, F. C. J. M.; Reinhoudt, D. N.; Moller, M.; Gittins, D. I. *Phys. Rev. Lett.* **2002**, *89*, 203002−1.
(23) Craig, D.; Thirunamachandran, T. *Molecular Quantum Electrodynamics*; Academic Press: London, 1984.
(24) Alivisatos, A. P.; Waldeck, D. H.; Harris, C. B. *J. Chem. Phys.* **1985**, *82*, 541−547.
(25) Johnson, P. B.; Christy, R. W. *Phys. Rev. B* **1972**, *6*, 4370−4379.
(26) Kreibig, U.; Genzel, L. *Surf. Sci.* **1985**, *156*, 678−700.
(27) Hövel, H.; Fritz, S.; Hilger, A.; Kreibig, U.; Vollmer, M. *Phys. Rev. B* **1993**, *48*, 18178−18188.
(28) Alvarez, M. M.; Khoury, J. T.; Schaaff, T. G.; Shafigullin, M. N.; Vezmar, I.; Whetten, R. L. *J. Phys. Chem. B* **1997**, *101*, 3706−3712.
(29) Turro, N. J. *Modern Molecular Photochemistry*; University Science Books: Sausalito, CA, 1991.
(30) Lewis, G. N.; Kasha, M. *J. Am. Chem. Soc.* **1945**, *67*, 994.
(31) 15-Dye: 5′ dye−C_6−CGT GTG AAT TCG TGC-3′. 15-Thiol: 5′ C_6S−S−C_6−GCA CGA ATT CAC ACG-3′. 30-Dye: 5′ dye-C_6−CGC CTA CTA CCG AAT TCG ATA GTC ATC AGC-3′. 30-Thiol: 5′ C_6S−S−C_6−GCT GAT GAC TAT CGA ATT CGG TAG TAG GCG-3′. 45-Dye: 5′ dye−C_6−CGT TCC GTG TGC ATA CTG AAT TCC GTG TTA CTC TTG CCA ACC TCG-3′. 45-Thiol: 5′ C_6S−S−C_6−CGA GGT TGG CAA GAG TAA CAC GGA ATT CAG TAT GCA CAC GGA ACG-3′.

(11) Weare, W. W.; Reed, S. M.; Warner, M. G.; Hutchison, J. E. *J. Am. Chem. Soc.* **2000**, *122*, 12890−12891.
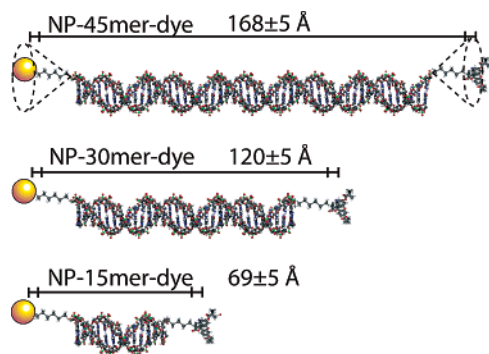
Figure 1. Scheme of DNA binding to a 1.5 nm Au NP. By varying the length of the DNA strand, the terminal dye fluorophore is separated from the Au NP by discrete distances (168, 120, and 69 Å.)

the integrated intensity under the curve for the PL peak, and $A_{control}$ is the absorption of the control sample at the peak of the dye. To eliminate absorption contribution from the NP in the calculation of the quantum efficiency of the dye, the value for A_{sample} is determined by subtracting the gold absorption profile from the absorption spectrum of the sample (NP−dsDNA−dye), yielding the fraction of light absorbed by only the dye at the wavelength of excitation.

Lifetime Measurements: Lifetimes are acquired using the output of a Nd:VO$_4$-pumped (Spectra-Physics Vanguard, 2 W, 532 nm, 76 MHz, 10 ps) R6G dye laser (Coherent 702-1). Cavity dumping of the dye laser to 1.9 MHz drops the pulse train to 1 pulse every 2 μs. In the case of FAM, the laser is frequency doubled for λ_{ex} = 300 nm and used as is at λ_{ex} = 600 nm for Cy5. Samples were excited with <1 μW at a right angle geometry relative to a Chromex 500is 0.5 m imaging monochromator with 50 g/mm grating and 0.5 nm resolution. Output of the monochromator is focused into a Hamamatsu C5680 streak camera operating at a 20 (FAM) or 10 ns window (Cy5). Lifetimes are measured by binning intensity versus time for a 20 nm spectral range about the λ_{em} maximum for the dye. Lifetime quenching is calculated by

$$Q_{eff} = 1 - \frac{\tau'}{\tau_0} \tag{5}$$

which compares the measured decay rate for a NP−dsDNA−dye system (τ') versus the observed decay rate for the identical dsDNA−dye in the absence of NP (τ_0).

Results

Figure 1 demonstrates the scheme of separating a donor fluorophore from the surface of a NP using three different lengths of dsDNA as a spacer, hereafter referred to as NP−dsDNA−dye. The distance from the center of the molecule to the metal surface is estimated by taking into account the C$_6$ linkers and the size of the fluorescent dye. The C$_6$ linkers on either side 5′ end contribute flexibility to the system, but due to the persistence length of dsDNA, ~90 nm,[12] and the fact that a d = 1.5 nm NP is smaller than the 2 nm footprint of dsDNA, it is very unlikely that the lengths of dsDNA used here would have the ability to wrap around or interact with the gold NP. The C$_6$ chain on the dye will produce a cone of probability for the separation distance, due to chain flexibility, and tend to randomize the dipole vector relative to the nanometal surface, so that the primary effect of the C$_6$ linker is ensuring an isotropic distribution of electronic dipoles.

Lifetimes: Figure 2 compares the lifetimes for both fluorescein (FAM, graph a) and Cy5 (graph b) at all three dsDNA spacer distances from the NP surface. The intensities have all
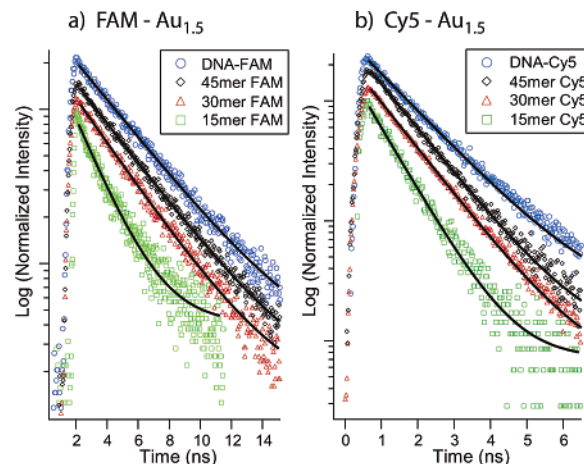

Figure 2. Lifetimes of the 15 bp (green), 30 bp (red), and 45 bp (black) NP−dsDNA−dye assemblies for FAM (a) and for Cy5 (b) relative to dsDNA−dye controls (blue, top). The data have been normalized and offset vertically for viewing. Single-exponential fits through the data are shown (−).
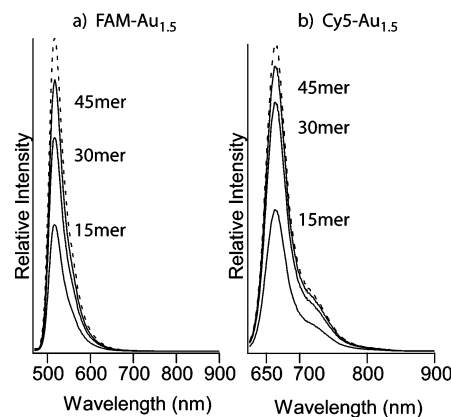

Figure 3. (a) Photoluminescence quenching of FAM PL intensity as a function of dsDNA spacer length. (b) Photoluminescence quenching of Cy5 dye as a function of spacer length. The top curve in both (a) and (b) (- - -) is a normalized control intensity.

been normalized at the peak and are displayed on a logarithmic graph vertically offset for comparison. The lifetime for each dye clearly decreases with decreasing distance to the surface of the metal sphere, displaying single-exponential decay kinetics fit using a Levenberg−Marquardt algorithm to minimize the residuals about the form: $I(t) = y_0 + I_0e^{-kt}$. This is the first-order rate law where y_0 is a linear offset, I_0 is the intensity at t = 0, and k is the rate of decay where $1/k = \tau_{obs}$. These observations suggest that not only is the sample purified from free dye but also that any variation in length caused by the C$_6$ spacer is not measurable for this system. All samples are compared to the appropriate dsDNA−dye strand in the absence of the NP (i.e., FAM-15mer-NP is compared to FAM-15mer); however, only a single dsDNA−dye strand is shown (top, blue) for comparison in Figure 2a,b. Using eq 5, the quenching efficiencies as measured by lifetime are listed in Table 1 along with the extracted (eq 1) and theoretical (eq 7) rates of energy transfer.

Photoluminescence: In Figure 3, the cw-PL quenching of FAM (Figure 3a) and Cy5 (Figure 3b) as a function of dsDNA spacer length is compared. The quantum efficiency of quenching for each sample was measured by comparison against a control dsDNA−dye in the absence of NP, using eq 4. Quenching
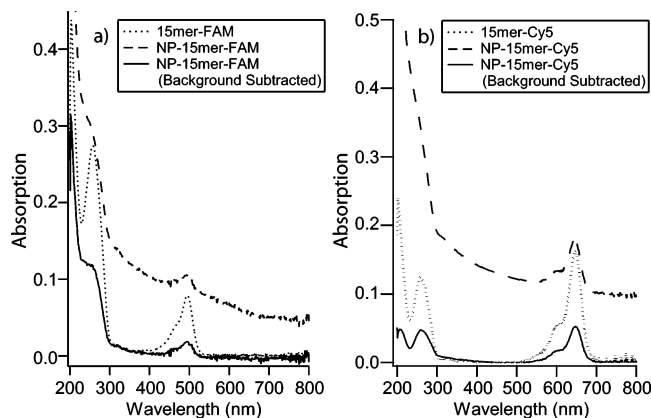
Figure 4. (a) Absorption and corrected spectra for the FAM−dsDNA−NP system and (b) absorption spectra and corrections for Cy5−dsDNA−NP. These spectra compare purified dye−dsDNA−NP (black, offset 0.05 au−FAM: 0.10 au−Cy5), dye−dsDNA in buffer (· · ·), and the background subtracted absorption spectrum of the dye−dsDNA−NP to correct for NP absorption (—).

efficiencies based on PL studies are tabulated in Table 1 versus different spacer lengths.

Absorption: Figure 4a shows absorption spectra for NP-15mer dsDNA−dye (black dashed lines, offset vertically), 15mer dsDNA−dye without NP (dotted lines), and the NP-15mer dsDNA−dye (solid line) after subtracting the absorption arising from the NP. The absorption for the difference spectra is not well resolved at the higher wavelengths, probably a result of unsatisfactorily corrected scattering.

Discussion

Development of the Model: A great deal of theoretical modeling[2,4,13−18] (this list is far from complete) has probed the behavior of a dye in which the molecular dipole is damped by the response of a nearby metal surface. The quenching of the fluorophore intensity must be related to a through-space mechanism involving only the dipole of the donor and some electronic property of the gold NP, which are most likely interactions with free electrons. The lack of an SPR band at the nanometal size used in this study suggests that the coherent behavior of electrons is diminished. This does not negate energy transfer to the metal surface but implies the lack of participation of the SPR or enhanced rates of energy transfer suggested over the plasmon bandwidth,[4,19] but not the ability of a metal to accept energy. This is an important point because, although a larger sized NP may accept energy more efficiently, the smallest NP possible is desired to be the least intrusive for a biological system.

Figure 5 illustrates the dipole projections for free electron scattering at the surface of a gold NP in the presence of an dipole-induced electric field. Any free electron traveling within the NP has the highest probability, geometrically speaking, of scattering normal to the surface as opposed to any other orientation due to the high curvature of a 1.5 nm gold NP. This would manifest in relaxing the dependence upon the overlap of projected dipoles between the donor and the acceptor.

The Gersten−Nitzan models[19−21] which have been used for modeling dipole−dipole interactions with the plasmon of gold NPs seem to have fallen short in describing both the distance dependence and efficiency of dye quenching.[5,22] The model of Persson and Lang, however, concerns itself primarily with

momentum and energy conservation in the dipole-induced formation of electron−hole pairs and is useful for modeling this system. According to this model, the rate of energy transfer is calculated by performing a Fermi golden rule calculation for an excited-state molecule depopulating with the simultaneous scattering of an electron in the nearby metal to above the Fermi level. However, in considering the conservation of momentum, the excitation of an electron−hole pair must coincide with an electron−electron, electron−phonon, or electron−surface potential scattering event.

The Persson model[3] states that the damping rate to a *surface* of a noble metal may be calculated by

$$k_{et} = 0.3\frac{\mu^2}{\hbar}\frac{\omega_{dye}}{\omega_F k_F d^4} \tag{6}$$

which can be expressed in more measurable parameters through the use of the Einstein A_{21} coefficient:[23]

$$A_{21} = \frac{\omega_{dye}^3}{3\epsilon_0\hbar\pi c^3}|\mu|^2$$

to give the following rate of energy transfer, in accordance with Coulomb's law ($1/4\pi\epsilon_0$):

$$k_{et} = 0.225\frac{c^3}{\omega_{dye}^2\omega_F k_F d^4}\frac{\Phi_{dye}}{\tau_{dye}} \tag{7}$$

where c is the speed of light, Φ_{dye} is the quantum yield of the donor (FAM = 0.8, Cy5 = 0.4), ω_{dye} is the angular frequency for the donor (FAM = 3.8×10^{15} s^{-1}, Cy5 = 2.91×10^{15} s^{-1}), ω_F is the angular frequency for bulk gold (8.4×10^{15} s^{-1}), and k_F is the Fermi wavevector for bulk gold (1.2×10^8 cm^{-1}). The d_0 value is a convenient value to calculate for a dye−metal system, yielding the distance at which a dye will display equal probabilities for energy transfer and spontaneous emission. For the Persson model, the d_0 value may be calculated by[32]

$$d_0 = \left(0.225\frac{c^3\Phi_{dye}}{\omega_{dye}^2\omega_F k_F}\right)^{1/4} \tag{8}$$

We calculate d_0 values of 76.3 and 73.0 Å for FAM and Cy5 dyes, respectively. The theoretical plot overlay of the data in Figure 6a,b is shown for comparison and is generated from the expression

$$Q_{Eff}(d) = 1 - \frac{1}{1 + \left(\frac{d_0}{d}\right)^4} \tag{9}$$

It is important to note that this model does not concern itself with the reflected field from the surface, which makes it convenient for the case of a metal NP where, in accordance with Ruppin's model,[4] it is assumed that the reflected field is negligible and does not interfere with the dipole field. For the validity of this model, we assume that the dipole is a point dipole separated from a metal sphere by a rigid distance and that every

---

(32) This equation is stated as a correction to a previous paper (Strouse, G. F. *J. Am. Chem. Soc.* **2005**, *127*, 3115) in which it was calculated in error to be 0.525.

Table 1. Measured Values for the Quantum Yield of Quenching Efficiency for the Three Strands of dsDNA Based on cw-PL Spectra (PL Q_{Eff}) and on Lifetime Quenching (τQ_{Eff})

	FAM, $\tau_0 = 3.53 \pm 0.10$ ns			Cy5, $\tau_0 = 1.30 \pm 0.10$ ns		
dsDNA strand distance (± 5 Å):	15 bp 69 Å	30 bp 120 Å	45 bp 167 Å	15 bp 69 Å	30 bp 120 Å	45 bp 167 Å
PL Q_{Eff}	0.45 ± 0.07	0.27 ± 0.06	0.06 ± 0.04	0.54 ± 0.06	0.19 ± 0.04	0.07 ± 0.03
τQ_{Eff}	0.47 ± 0.04	0.13 ± 0.03	0.04 ± 0.02	0.41 ± 0.05	0.10 ± 0.04	0.02 ± 0.04
calculated k_{et} (s^{-1})^a	2.55×10^8	4.9×10^7	1.3×10^7	4.87×10^8	8.5×10^7	9.72×10^6
theoretical k_{et} (s^{-1})^a	4.3×10^8	4.7×10^7	1.2×10^7	3.3×10^8	3.6×10^7	8.6×10^6

^{a} The calculated and theoretical rates of energy transfer to the metal surface are calculated using eqs 3 and 7, respectively.
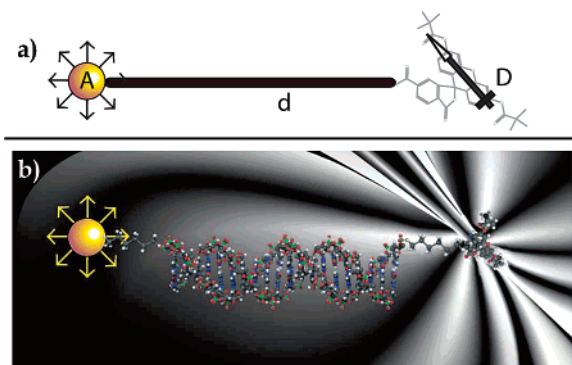
Figure 5. (a) Graphic representation of a donor dye−nanometal acceptor pair separated by dsDNA approximated as a rigid rod of length, *d*. The donor is treated as a localized dipole, and the acceptor is assumed to have overlap at all stearadians. (b) Pictorial representation of a gold NP in an idealized electric field of a nearby molecular dipole. All surface dipole scattering events associated with the free electrons of the gold are shown perpendicular to the surface, which are predicted to be the dominant contributors to the NSET process.
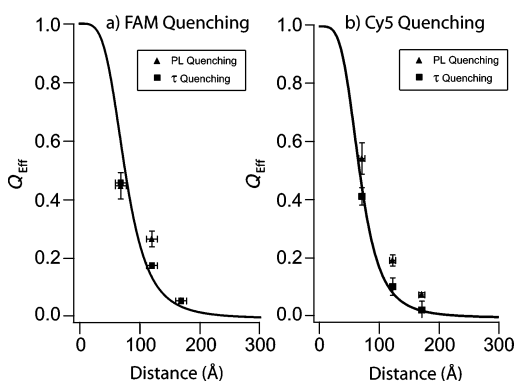
Figure 6. Quenching data for FAM (a) and Cy5 (b) based upon photoluminescence (▲) and lifetimes (■) overlaid on top of a theoretical curve generated using eq 9.

fluorophore has an acceptor NP associated with it. This assumption is made practical in the material conjugation by saturating the dsDNA with acceptor NP and using less than a stoichiometric amount of donor-labeled strand. Monoexponential lifetimes support the assumption that every donor is located at a rigid distance from the acceptor.

Alivisatos was successful in adapting the Persson model to describe energy transfer from biacetyl donors to a Ag(111) surface with good agreement to experimental data.[24] For their system, it was concluded that the dipole damping as a result of both bulk and surface electron scattering was important. However, a metal particle on the scale of 1.5 nm, being well below the electron mean-free path (∼430 Å for gold[25]), will not show bulk electron scattering effects. Instead, it is expected

that the overwhelming majority of electron scattering events are associated with the surface potential.

Figure 6 compares the experimentally observed quenching efficiencies of a 1.5 nm NP as measured by PL and calculated using eq 4 and also as measured by luminescence lifetime using eq 5. A theoretical curve calculated using eq 9 is overlaid for comparison to theory. Although eqs 7 and 8 use bulk gold parameters, the model fits surprisingly well with the experimentally measured values and, particularly, with the rates of energy transfer reported in Table 1. The photoluminescence characterization seems to overestimate slightly the theoretical quenching values, whereas the lifetimes are in excellent agreement with the model. Because the measurement of relative quantum efficiencies via PL spectra is prone to error in the form of fluctuations in lamp intensity or the ability to accurately measure absorption, the PL quenching efficiencies are considered less reliable than lifetime measurements. Fluorescence lifetimes avoid the accumulated error associated with the use of multiple instruments, which increases our confidence in their measurement. Lifetimes are very sensitive to the presence of quenching processes and give insight into the number of quenching processes taking place. The lifetimes measured here not only suggest that quenching is occurring due to a single energy transfer event (decreased single-exponential lifetime) but also suggest that the slope of the theory may be correct.

The absorption characteristics of gold NPs have been studied extensively, and attempts to fit theory with experimental data have furnished a rich description of the electronic and optical properties of metal NPs. Attempts to model the absorption for gold NPs below 20 nm diameter, in particular, the bandwidth and position of the SPR band, require the incorporation of an enhanced surface potential scattering term in the Drude dipole approximation.[26,27] Whetten was successful in adapting this model to calculate the absorption spectra of gold NPs from *d* = 1.4−3.2 nm, where they advance the theory that thiol ligands donate electron density into the NP.[28] In this regard, the use of NPs as energy acceptors may actually enhance the quenching efficiency of a metal surface and explain the somewhat unexpected efficiency of quenching by a 1.5 nm NP. The increased electron density and surface scattering enhance the probability of energy transfer via the Persson model, accounting for the good agreement between the data shown here and the theoretical model.

Monitoring k_r: The observed quenching behavior of a molecular dye at a specified distance above a metal surface has been explained previously by a perturbed radiative rate.[5] Neither lifetime nor PL data alone will give evidence toward the true origin of the observed quenching because either can be explained by the radiative rate or energy transfer models. An absorption